ChemComm

Accepted Manuscript

This article can be cited before page numbers have been issued, to do this please use: S. Biswas, B. Dutta, A. Mannodi-Lanakkithodi, R. Clarke, W. Song, R. Ramprasad and S. L. Suib, *Chem. Commun.*, 2017, DOI: 10.1039/C7CC06097A.

This is an Accepted Manuscript, which has been through the Royal Society of Chemistry peer review process and has been accepted for publication.

Accepted Manuscripts are published online shortly after acceptance, before technical editing, formatting and proof reading. Using this free service, authors can make their results available to the community, in citable form, before we publish the edited article. We will replace this Accepted Manuscript with the edited and formatted Advance Article as soon as it is available.

You can find more information about Accepted Manuscripts in the author guidelines.

Please note that technical editing may introduce minor changes to the text and/or graphics, which may alter content. The journal's standard Terms & Conditions and the ethical guidelines, outlined in our author and reviewer resource centre, still apply. In no event shall the Royal Society of Chemistry be held responsible for any errors or omissions in this Accepted Manuscript or any consequences arising from the use of any information it contains.

ROYAL SOCIETY OF CHEMISTRY

rsc.li/chemcomm

View Article Online
DOI: 10.1039/C7CC06097A

Journal Name

COMMUNICATION

Heterogeneous Mesoporous Manganese/Cobalt Oxide Catalyst for Selective Oxidation of 5-hydroxymethylfurfural to 2,5-diformylfuran†

Sourav Biswas[a,†], Biswanath Dutta[b,†], Arun Mannodi-Lanakkithodi[c], Ryan Clarke, Wenqiao Song[b], Rampi Ramprasad[c] and Steven L. Suib[b,c*]

www.rsc.org/

We report a heterogeneous catalytic protocol for oxidation of 5-hydroxymethylfurfural (HMF) to 2,5-diformylfuran (DFF) using mesoporous manganese doped cobalt oxide material. The absence of precious metals and additives, use of air as the sole oxidant, easy isolation of products, along with proper catalyst reusability make our catalytic protocol attractive for selective oxidation of HMF to DFF.

Due to the rapid exploitation of the fossil feedstock, there are demands for sustainable alternative energy and new chemical feed stocks.[1,2] Even though renewable energy sources (such as solar, geothermal and wind) have gained much attention recently, they are unable to produce petroleum based organic building blocks which are required for producing plastics and fine-chemicals.[3,4] Biomass resources are renewable, abundant and contain skeletal carbon atoms and have been found to be the only source of sustainable feedstocks for the chemical and fuel industries.

5-hydroxymethylfurfural (HMF) is one such promising platform molecule, derived from acid catalyzed dehydration of C6 based carbohydrates,[5–7] which has two different functional groups (hydroxyl and aldehyde) and is known for versatile applications as fine chemicals and liquid fuels.[4] Oxidation of HMF can lead to the formation of various industrially value-added products such as 2,5-diformyl furan (DFF), 5-hydroxymethyl-2-furan carboxylic acid (HMFCA), 5-formyl-2-furancarboxylicacid (FFCA) and 2, 5-furan-dicarboxylicacid (FDCA).[8–11] Among those, DFF has versatile applications in the synthesis of polymers,[12] pharmaceuticals,[13] and other value added products. However, the presence of highly react-

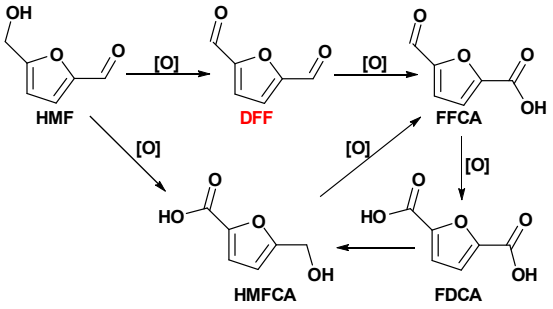

Figure 1. Various routes to synthesize different HMF derivatives.

-ive α, β-unsaturated aldehyde in HMF makes selective oxidation of HMF to DFF very difficult. Both homogeneous[14,15] and heterogeneous[16,17] catalysts have been explored for oxidation of HMF to DFF. Most homogeneous catalysts suffer from reusability issues, whereas heterogeneous procedures display comparatively lower activity and selectivity.[16] In some cases, precious metal catalysts have been employed for this selective oxidation.[18–20] There are few reports on manganese oxide based catalysts for selective oxidation of HMF to DFF.[21] However, either the use of molecular oxygen or high air pressure (15 atm) are required to achieve catalytic efficiency, which limit practical applications. Therefore, the development of a cost-effective, selective and efficient catalytic procedure for the synthesis of HMF to DFF under aerobic and atmospheric conditions is highly desirable.

In 2013, a series of mesoporous materials were developed by our group using inverse-micelle templated evaporation induced self-assembly methods.[22] Both, mesoporous cobalt oxide and mesoporous manganese oxide materials synthesized by this method, have displayed excellent activity in different liquid phase and gas phase oxidation reactions.[23, 24] The inter-dependence of redox cycles with labile lattice oxygen molecules are believed to be crucial factors for these catalytic systems. Surface defects caused by dopants are known to enhance catalytic activity of metal oxides by increasing the lattice oxygen content. However, this effect was never evaluated using two equally active metal oxide systems.

[a] Dr. S. Biswas,[†]
Department of Chemistry, University of Wisconsin-Madison, 1101 University Avenue, Madison, Wisconsin 53706, USA.
[b] B. Dutta,[†] Dr. W. Song, Ryan Clarke, Prof. S. L. Suib.
Department of Chemistry, University of Connecticut, 55 North Eagleville Road, Storrs, Connecticut 06269-3060, USA.
[c] A. Mannodi-Lanakkithodi, Prof. R. Ramaprasad, Prof. S. L. Suib.
Institute of material science, University of Connecticut, Storrs, Connecticut 06269-3060, USA.
[†] These authors contributed equally.

View Article Online
DOI: 10.1039/C7CC06097A

Herein, we present our effort of designing an efficient catalytic system using mesoporous manganese incorporated cobalt oxide (meso Mn-CoOx) for selective oxidation of HMF to DFF. The oxidation reaction, being inefficient for both manganese and cobalt oxides, were tested with different Co-Mn mixed metal oxide catalysts. The doping of manganese oxide in cobalt oxide was found to perform better than the reverse. The beneficial effect of Mn in the cobalt oxide structure for designing an efficient catalyst will be discussed in detail. Additionally, structure-activity relationships were explored aided by DFT computations to evaluate reaction pathways over these catalysts.

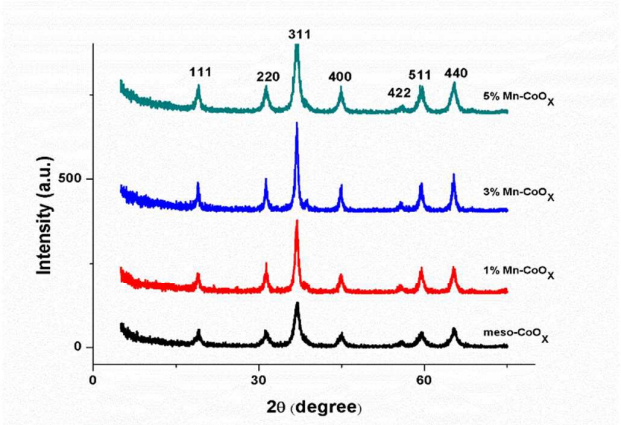

Figure 2. Powder X-ray diffraction (PXRD) of meso Mn/ CoOx at different Mn/Co ratio. (the diffraction patterns correspond to tricobalt tetraoxide).

The meso-CoOx and all Mn doped Meso-CoOx materials were found to be crystalline (**Figure 2**). The PXRD patterns indicate the Co_3O_4 crystal structure. No other crystalline phase was observed for the Mn doped materials confirming little phase segregation. The N_2 sorption isotherms displayed typical Type IV adsorption isotherms, which denote the mesoporosity of the materials (**Figure S1**). The reduction of surface area due to Mn doping is probably due to partial pore-blocking or formation of a second low surface area phase. However, no direct correlation of surface area reduction and Mn dopant amount was observed. All the materials possessed a monomodal mesoporous size distribution with pore sizes between 5.2 to 17 nm (**Figure S1 and Table S1**).

Table 1 gives catalytic data for aerobic oxidation of HMF to DFF using different manganese and cobalt oxide catalysts. The bare mesoporous cobalt oxide (meso CoOx), and manganese oxide (meso MnOx) materials displayed low yields of DFF (**Table 1, Entry 1 and 2**), albeit high selectivity. An enhancement in the activity (while preserving high selectivity) was observed when Mn was introduced in mesoporous cobalt oxide materials. The sharp increase in conversion was noticed under similar conditions and reached saturation with only 5 % manganese doping (**Table 1, Entry 3 - 5**). Further increase in manganese content did not have any significant effect on conversion (**Table 1, Entry 6 and 7**). Notably, the reaction did not produce any product under catalyst-free conditions (**Table 1, Entry 8**).

Table 1. Comparison of catalysts on HMF oxidation [a]

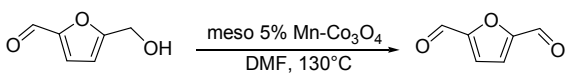

Entry	Catalyst	Conversion [b] (%)	Selectivity [b] (%)	TOF [c] (h^{-1})
1	Meso CoOx	18	98	6×10^{-4}
2	Meso MnOx	13	> 99	4.6×10^{-4}
3	Meso 1% Mn/CoOx	24	96	0.26
4	Meso 3% Mn/CoOx	40	95	0.15
5	Meso 5% Mn/CoOx	80 (71)	96	0.18
6	Meso 10% Mn/CoOx	78	95	0.09
7	Meso 20% Mn/CoOx	77	96	0.04
8	No catalyst	< 1	> 99	N/A

[a] **Reaction conditions:** HMF (0.50 mmol), catalyst (50 mg), DMF (3 mL) at 130°C, 4 h. [b] Conversions and selectivity were determined by GC-MS based on concentration of HMF (*see* GC-MS in **Figure S9**). [c] TOF = TON/ time (h). TON= no of moles of HMF converted to the product per mole of catalyst. In parenthesis, refers to the yield of isolated product (*see* NMR in **Figure S10**).

While optimizing the catalyst loading, a continual increase in performance was observed with increasing catalyst loading (**Figure S2**). These results signify that the system had no limitations due to mass transfer or limited adsorption sites. The reaction was also screened with different solvents of varying polarity, where N, N'-dimethylformamide (DMF) emerged as the best solvent (**Table 2**). High DFF yield was also obtained using water as solvent, which highlighted the practical applications of our process using 'green conditions'.

Table 2. Survey of solvents for oxidation of HMF to DFF [a]

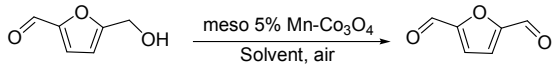

Entry	Solvent	Temp. (°C)	Conv. [b] (%)	Selectivity [b] (%)
1	DMF	130	80	96
2	Toluene	110	<1	>99
3	Acetonitrile	80	15	>99
4	1,4-dioxane	100	<1	95
5	Water	100	70	>99

[a] **Reaction conditions:** HMF (0.50 mmol), Meso 5% Mn/CoOx (50 mg), solvent (3 mL) at the respective boiling point temperatures, 4 h. [b] Conversions and selectivity were determined by GC-MS based on concentration of HMF.

No improvement of reaction rate was observed under a pure oxygen atmosphere rather than air. However, a decrease of activity was found in nitrogen environment (**Table S2, Entry 1, 2 and 3**). Addition of one equivalent of base (K_2CO_3) (**Table S2, Entry 4**)

View Article Online
DOI: 10.1039/C7CC06097A

resulted in an increase of turnover due to the enhanced deprotonation, facilitated by the base. However, the conversion under this base mediated process did not increase significantly with just an oxygen environment. Hence, a reaction using DMF as solvent at 130 °C, under oxygen environment and in the presence of the catalyst (meso-5%-Mn-CoOx-250) was chosen to be best optimal reaction conditions.

In heterogeneous catalysis, leaching of active metals in solution and deactivation of the active sites due to adsorption or aggregation are very common issues. To verify if the active metals leached out during the reaction, a hot filtration test was carried out (**Figure S3**). In that experiment, the catalyst was separated from the reaction system by a simple filtration method after 40 minutes (at about 20% conversion) and the filtrate was kept under the same reaction conditions for another 60 minutes. No further improvement in conversion of HMF was achieved. Further analysis of the filtrate by atomic adsorption spectroscopy (AAS) revealed the presence of negligible quantities of Mn and Co (<1 ppm). To determine reusability, the catalyst was retrieved from the reaction mixture by simple filtration and washed with excess DMF and ethanol. Prior to reuse, the catalyst was reactivated at 250 °C for 30 min to remove any adsorbed species. Similar pre-and post-reaction treatments were done to the catalyst for another five cycles, until the conversion dropped by ~23 % of its initial activity (**Figure S4, a**). An X-ray diffraction study on the catalyst after the 6^{th} cycle, confirmed the preservation of the crystalline nature of the catalyst without any noticeable change (**Figure S4, b**). Therefore, our catalyst can be considered to be truly heterogeneous, stable, and reusable.

The kinetic aspects of the reaction were determined by conducting a time-dependent study (**Figure S5**). A first order rate equation was derived with respect to HMF with a rate constant of 5.8×10^{-3} s^{-1} (**Figure S6**). To estimate the apparent activation energy of the reaction, a series of time-dependent reactions were performed in the temperature range of 80 –140 °C. This resulted in an activation energy (E_a) of 5.79 kcal. mol^{-1}, from the Arrhenius equation (**Figure S7**).

To study possible structure-activity relationships, a series of characterization techniques such as H_2-TPR (temperature programmed reduction) and XPS (X-ray photoelectron spectroscopy) were performed. Generally, metal oxide based catalytic systems operate by a Mars-Van-Krevelen mechanism, which involves an exchange between aerial and lattice oxygen.[25]Therefore, the activity of the catalyst depends on the mobility and accessibility of lattice oxygen, which in turns relates to M-O bond length. The presence of one electron in the antibonding e_g orbital (e^1g) of Mn^{3+} species, results in an elongation of Mn-O bonds due to Jahn–Teller (J–T) distortion.[26] XPS data revealed a sharp increase in Mn^{3+} and lattice oxygen content, with increasing Mn doping percentages. The most active 5% Mn-CoOx has the maximum lattice oxygen content and highest amounts of Mn^{3+} species.

Along with the metal oxidation states, the mobility and accessibility of lattice oxygen are also important. From redox perspectives, an easily reducible material provides an increase in mobility and ease of removal of lattice oxygen species. **Figure S8** displays the H_2-TPR profile of the meso CoOx materials. Three different reduction peaks were observed corresponding to reduction of surface adsorbed species (labile oxygen) at 25°C to 250°C, Co^{3+} reduction at 260°C to 350°C and Co^{2+} reduction at higher temperature.[24] The highest activity of meso 5%Mn-CoOx can be rationalized by the lowest reduction temperature for lattice oxygen. According to the Mars-Van-Krevelen mechanism, electron transfer from adsorbed species (alkoxide) to metal centers reduces the metal. Therefore, the easier reduction of the metal center the more active is the material. This can be reinforced by the fact that the lowest Co^{3+} reduction temperature of meso 5% Mn/CoOx was the reason for the high catalytic activity.

High surface area and nano-crystallinity of these materials are also considered to be critical for achieving excellent efficiency. High surface area provided better access to the catalytically active sites to promote activity, whereas nano-crystallinity ensured the availability of the labile lattice oxygens.[23, 27] The best active material, namely, 5 % meso Mn-CoOx has high surface area (121 m^2g^{-1}), which also contributed to the high catalytic activity. Moreover, the well-defined porous network of the material provides facile diffusion and mass transport of the HMF molecules, which is essential for heterogeneous catalysis.

Based on these observations, we propose a mechanism of HMF oxidation over cobalt oxide surfaces (**scheme S1**). Initially, a radical scavenger (2,6-di-tert-butyl-4-methylphenol) was introduced to the reaction mixture, to trap the radical intermediate, if formed. However, the absence of such intermediates, suggests a radical free pathway. The reaction starts with O-H bond dissociation on the catalyst surface, followed by the protonation of lattice oxygen. This can be rationalized by the increase of activity by introduction of base. The alkoxide formed at this step reduced the metal center. In the second step, a deprotonation from α-CH_2, led to the formation of product (**DFF**). The consecutive reductions of the metal oxide surface, led to release of a molecule of H_2O_2 which eventually decomposed to water and oxygen.[28] During catalysis, the reduced metal species can be re-oxidized by oxygen molecules. Thus, an aerobic atmosphere should play a critical role in replenishing the vacancies made by lost lattice oxygen. This turned out to be consistent with the observed decrease of catalytic efficiency under a nitrogen atmosphere (45 % conversion), compared to aerobic conditions (55 % conversion). A post reaction (under nitrogen atmosphere) XPS analysis on the catalyst **Table S3**), also revealed a significant decrease (20 %) of lattice oxygen (O_L) compared to the material before reaction (70.56 %). This indicates the existence of oxygen vacancies due to incomplete replenishment under nitrogen atmosphere and further supported the above-mentioned experimental findings.

To further validate the reaction mechanism, quantum-mechanical computations were performed using density functional theory (DFT) as implemented in the Vienna ab initio simulation package (VASP).[29] The Perdew, Burke and Ernzerhof (PBE) electron exchange-correlation function[30] was used along with the projector

View Article Online
DOI: 10.1039/C7CC06097A

augmented-wave (PAW) frozen core potentials[31] to estimate the total energies of all the different configurations, from the reactants to intermediates to products. Our primary target was to find out the order of bond dissociation (C-H and O-H) and energies involved with corresponding intermediates.

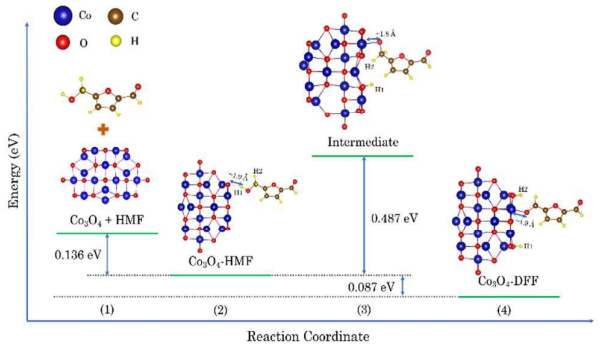

Figure 2. Energy profile of the reaction in gas phase, as determined by DFT calculations.

DFT calculations were performed on the (311) cobalt oxide surface. A DFT energy profile for the reaction in the gas phase is shown in **Figure 2**. The relative energies [kcal mol^{-1}] are based on the summation of the representative total energies E_{tot} of all species. According to these calculations, HMF was stabilized on the surface of the catalyst prior to undergoing O-H bond dissociation. In the next step, a C-H bond dissociated to produce DFF. Moreover, the energy associated with the O-H bond dissociation was calculated to be higher than the C-H bond dissociation, making this the rate determining step.

In summary, we developed a cost-effective heterogeneous catalytic procedure, operable under mild reaction conditions, for selective oxidation of HMF to DFF using readily abundant and reusable manganese doped cobalt oxide materials. Under optimized reaction conditions we used DMF as the solvent. The catalyst also showed high activity (70 % conversion) in water, which highlighted the practical applicability of our process. The catalytic protocol circumvents the use of additives and precious metals. Our experimental and computational studies provide a reaction mechanism, which involves an O-H bond dissociation followed by C-H abstraction over the catalyst surface. The involvement of surface active Mn^{3+} and O_L species were confirmed to be critical for our systems. Additionally, high surface area, nano-crystallinity, and a uniform porous network of the materials are also believed to be important factors for the catalytic efficiency of these materials.

S.L.S thanks the US Department of Energy, Office of Basic Energy Sciences, Division of Chemical, Biological and Geological Sciences under grant DE-FG02-86ER13622.A000 for support of this research.

Notes and references

1 S. E. Davis, A. D. Benavidez, R. W. Gosselink, J. H. Bitter, K. P. de Jong, A. K. Datye and R. J. Davis, *J. Mol. Catal. A Chem.*, 2014, **388**, 123–132.
2 C. Dupont, R. Chiriac, G. Gauthier and F. Toche, *Fuel*, 2014, **115**, 644–651.
3 J. N. Chheda, Y. Roman-Leshkov and J. A. Dumesic, *Green Chem.*, 2007, **9**, 342–350.
4 T. Thananatthanachon and T. B. Rauchfuss, *Angew. Chem. Int. Ed.*, 2010, **49**, 6616–6618.
5 Y. Roman-Leshkov, *Science (80-.).*, 2006, **312**, 1933–1937.
6 A. Corma Canos, S. Iborra and A. Velty, *Chem. Rev.*, 2007, 107, 2411–2502.
7 D. J. Chadderdon, L. Xin, J. Qi, Y. Qiu, P. Krishna, K. L. More, W. Li, J. A. Lopez-Sanchez, S. H. Taylor, D. W. Knight, C. J. Kiely, G. J. Hutchings and G. J. Hutchings, *Green Chem.*, 2014, **16**, 3778–3786.
8 S. E. Davis, B. N. Zope, R. J. Davis, R. J. Davis and R. J. Davis, *Green Chem.*, 2012, **14**, 143–147.
9 W. P. Dijkman, D. E. Groothuis and M. W. Fraaije, *Angew. Chem. Int. Ed.*, 2014, **53**, 6515–6518.
10 Z. Zhang, B. Liu, K. Lv, J. Sun and K. Deng, *Green Chem.*, 2014, **16**, 2762–2770.
11 Z. Du, J. Ma, F. Wang, J. Liu and J. Xu, *Green Chem.*, 2011, **13**, 554–557.
12 C. Moreau, M. N. Belgacem and A. Gandini, *Top. Catal.*, 2004, **27**, 11–30.
13 A. A. Rosatella, S. P. Simeonov, R. F. M. Frade and C. A. M. Afonso, *Green Chem.*, 2011, **13**, 754–793.
14 J. Ma, Z. Du, J. Xu, Q. Chu and Y. Pang, *ChemSusChem*, 2011, **4**, 51–54.
15 W. Partenheimer and V. V. Grushin, *Adv. Synth. Catal.*, 2001, **343**, 102–111.
16 J. Nie, J. Xie and H. Liu, *J. Catal.*, 2013, **301**, 83–91.
17 K. Ghosh, R. A. Molla, M. A. Iqubal, S. S. Islam and S. M. Islam, *Appl. Catal. A Gen.*, 2016, **520**, 44–52.
18 M. A. Lilga, R. T. Hallen and M. Gray, *Top. Catal.*, 2010, **53**, 1264–1269.
19 A. Takagaki, M. Takahashi, S. Nishimura and K. Ebitani, *ACS Catal.*, 2011, **1**, 1562–1565.
20 C. A. Antonyraj, J. Jeong, B. Kim, S. Shin, S. Kim, K.-Y. Lee and J. K. Cho, *J. Ind. Eng. Chem.*, 2013, **19**, 1056–1059.
21 Z.-Z. Yang, J. Deng, T. Pan, Q.-X. Guo and Y. Fu, *Green Chem.*, 2012, **14**, 2986–2989.
22 A. S. Poyraz, C.-H. Kuo, S. Biswas, C. K. King'ondu and S. L. Suib, *Nat. Commun.*, 2013, **4**, 1–10.
23 S. Biswas, B. Dutta, K. Mullick, C.-H. Kuo, A. S. Poyraz and S. L. Suib, *ACS Catal.*, 2015, **5**, 4394–4403.
24 W. Song, A.S. Poyraz, Y. Meng, Z. Ren, S.Y. Chen, and S. L. Suib, *Chem. Mater.*, 2014, **26(15)**, 4629–4639.
25 C. Doornkamp, V. Ponec and H. Knozinger, *J. Mol. Catal. A Chem.*, 2000, **162**, 19–32.
26 U. Maitra, B. S. Naidu, A. Govindaraj and C. N. R. Rao, *roceedings Natl. Acad. Sci. United States Am.*, 2013, **110**, 11704–7.
27 S. Biswas, A. S. Poyraz, Y. Meng, C.-H. Kuo, C. Guild, H. Tripp and S. L. Suib, *Appl. Catal. B Environ.*, 2015, **165**, 731–741.
28 V. D. Makwana, Y. Son, A. R. Howell and S. L. Suib, *J. Catal.*, 2002, **52**, 46–52.
29 G. Kresse and J. Hafner, *Phys. Rev. B*, 1993, **47**, 558–561.
30 É. D. Murray, K. Lee and D. C. Langreth, *J. Chem. Theory Comput.*, 2009, **5**, 2754–2762.
31 P. E. Blöchl, *Phys. Rev. B*, 1994, **50**, 17953–17979.

View Article Online
DOI: 10.1039/C7CC06097A

Table of Content